

Prospective Analysis of a Novel Endobronchial Augmented Fluoroscopic Navigation System for Diagnosis of Peripheral Pulmonary Lesions

Michael A. Pritchett, DO, MPH

Background: Navigational bronchoscopy has improved upon traditional bronchoscopy to identify suspicious pulmonary lesions, but wide variability exists in the diagnostic yield of various modalities. The aim of this study was to measure localization accuracy and diagnostic yield of a novel endobronchial augmented fluoroscopic navigation system (first-generation LungVision system) for peripheral pulmonary lesions (PPLs).

Methods: This prospective single-center study included adults undergoing guided bronchoscopy to evaluate PPLs. Preprocedure computed tomography (CT) images were obtained, and planning software calculated a pathway to the lesion. A flexible bronchoscope was used to navigate along the pathway overlaid on the intraprocedural fluoroscopic image. When real-time display indicated the catheter tip had reached the lesion, cone-beam computed tomography (CBCT) was used to measure the actual location of the tip. Biopsy and rapid on-site cytopathologic evaluation were performed.

Results: Fifty-one patients were included in the analysis. The median lesion diameter was 18.0 mm (range: 7.0 to 48.0 mm). Localization success was 96.1%. The average distance between lesion location as shown by LungVision augmented fluoroscopy and actual location measured by CBCT was 5.9 mm (range: 2.1 to 10.0 mm). Diagnostic yield at the index procedure was 78.4%. Diagnostic accuracy assessed at 12 months follow-up was 88.2%. Average CT-to-body divergence was 14.5 mm (range: 2.6 to 33.0 mm) from preprocedure CT to intraprocedural CBCT images.

Conclusion: Augmented fluoroscopy for navigation and biopsy of PPLs with the LungVision system showed a high localization success rate and corresponding high diagnostic yield. Navigation and biopsy with real-time visualization can improve diagnostic yield for PPLs.

Key Words: bronchoscopy, lung cancer, lung lesion, peripheral lesion, guided bronchoscopy

(*J Bronchol Intervent Pulmonol* 2020;00:000–000)

Early-stage identification and treatment of non-small-cell lung cancer increases 5-year survival rates dramatically, from 19%¹ to 70%-90% for small, localized lesions (stage I).² Efforts to detect early-stage lung cancer, when it is most treatable, have relied heavily on diagnosis of peripheral pulmonary lesions (PPLs) using bronchoscopy, with mixed success.^{3,4} The variability in outcomes arises from the challenges of localizing the lesion in the complex and dynamic environment of the lung, which is continually moving due to breathing motion, physiological changes, and distortion of the anatomy by the catheter, scope or biopsy tools themselves. Bronchoscopy modalities that use a planned navigation pathway to the lesion rely on preoperative computed tomography (CT) images that do not accurately reflect the physical state of the lung at the time of the procedure.

Navigational modalities, including virtual bronchoscopy and electromagnetic navigation bronchoscopy (ENB), have increased diagnostic yields (55.7% to 73.8%^{5,6}) compared with traditional bronchoscopy (37%).⁷ Two large multicenter studies have evaluated diagnostic yield of ENB in a real-world setting. The AQUiRE registry, which evaluated standard bronchoscopy alone or in combination with radial probe endobronchial ultrasound (R-EBUS) and ENB in 581 patients at 15 centers, reported a diagnostic yield of 38.5% for ENB alone and 47.1% when combined with R-EBUS, using a conservative definition of diagnostic yield that includes only malignant and confirmed benign lesions at the index procedure.⁸ The NAVIGATE study of ENB in 1215 patients in 29 centers reported a 12-month diagnostic yield of

Received for publication February 12, 2020; accepted June 23, 2020.
From the FirstHealth Moore Regional Hospital and Pinehurst Medical Clinic, Pinehurst, NC.

Disclosure: Medtronic—speaking, consulting, research; Auris—speaking; BodyVision—consulting, speaking, research; Intuitive—research, speaking, consulting; Philips—research; Biodesix—speaking, research; AstraZeneca—consulting, speaking; Boehringer-Ingelheim—speaking; United Therapeutics—speaking, research; Actelion—speaking research; Inivata—research; Boston Scientific—consulting; OncoSec—consulting; Johnson & Johnson/NeuWave—consulting, speaking, research; Ambu—consulting.

Reprints: Michael A. Pritchett, DO, MPH, FirstHealth Moore Regional Hospital and Pinehurst Medical Clinic, Pinehurst, NC 28374 (e-mail: mpritchett@pinehurstmedical.com).

Copyright © 2020 The Author(s). Published by Wolters Kluwer Health, Inc. This is an open-access article distributed under the terms of the Creative Commons Attribution-Non Commercial-No Derivatives License 4.0 (CCBY-NC-ND), where it is permissible to download and share the work provided it is properly cited. The work cannot be changed in any way or used commercially without permission from the journal.

DOI: 10.1097/LBR.0000000000000700

73%, defined as malignant and benign lesions as well as indeterminate lesions confirmed as benign after 12 months follow-up.⁹

Traditional bronchoscopy combined with cone-beam computed tomography (CBCT) to acquire 3D imaging of the patient's lung and identify lesion location, as well as location and orientation of the catheter or biopsy tools, has shown a high localization rate of 91% but a diagnostic yield of only 70%.¹⁰ In a recent single-center retrospective analysis, CBCT with augmented fluoroscopy in conjunction with ENB improved diagnostic yield to 83.7%, even for very small lesions (median diameter: 16 mm), with diagnostic accuracy of 93.5%.¹¹

We assessed localization success and diagnostic yield of a novel navigation system that enables endobronchial augmented fluoroscopic navigation to PPLs with real-time visualization of the lesion during biopsy. We hypothesized that this approach would be safe and feasible, could improve nodule localization and potentially improve diagnostic yield.

MATERIALS AND METHODS

We conducted a prospective, single-center, single-arm study of the safety and feasibility of guided bronchoscopy using the first-generation LungVision system (Body Vision Medical Ltd, Israel) for diagnosis of suspicious PPLs at FirstHealth Moore Regional Hospital (Pinehurst, NC) between January 2017 and October 2018. Adult patients with peripheral lung nodules (ie, surrounded by normal aerated lung, not visible endobronchially and located beyond the segmental bronchus) identified on CT, for whom a guided bronchoscopy was felt to be necessary were eligible for inclusion, regardless of lesion size, location or presence of a bronchus sign. Patients with any prior lung resection or lung transplantation were excluded. The LungVision system comprises software and hardware connected to a fluoroscope (Fig. 1) and a location board with fluoroscopically visible markers that is placed under the patient's thorax and allows the system to perform geometrical computations. The system provides real-time enhancement of fluoroscopic-guided biopsy of PPLs

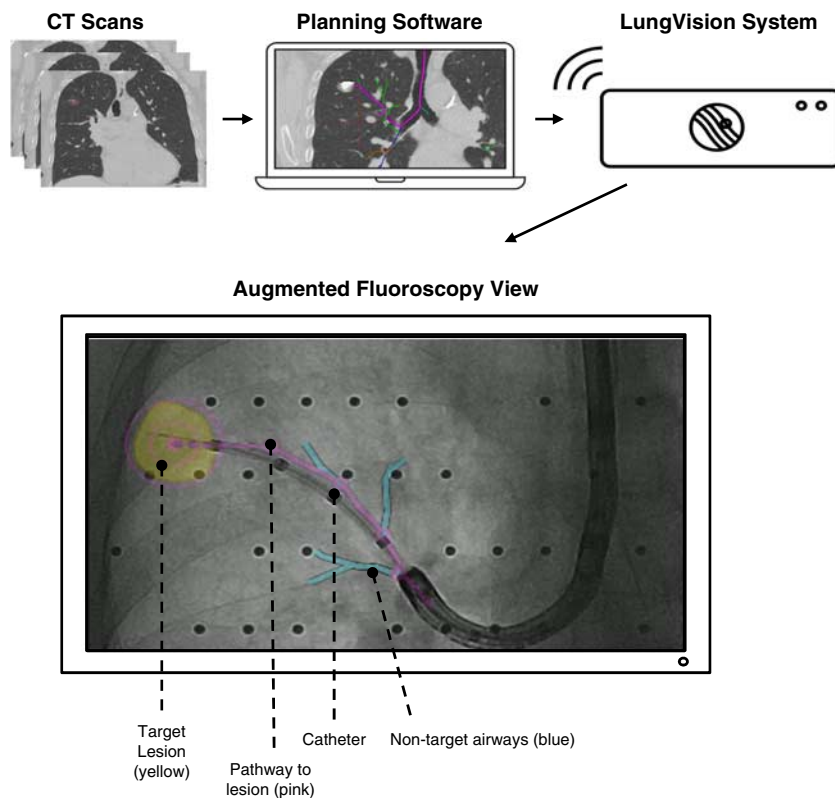


FIGURE 1. The LungVision System. The LungVision system integrates information from preprocedural computed tomography (CT) imaging into augmented fluoroscopic images. Data from the CT scan is imported into the planning software and the physician is able to identify the lesion and select a preferred navigation pathway to the lesion. A location board with fluoroscopically visible markers placed under the patient's thorax allows the system to perform geometrical computations. The system presents real-time visualization of the airways and location of the pulmonary lesion during transbronchial navigation and biopsy.

using previously acquired CT information to improve navigation to the lesions. The study protocol was approved by the Institutional Review Board (WIRB, IRB Registration number IRB00000533), and informed consent was obtained from all patients before the procedure.

A single pulmonologist performed all procedures under general anesthesia in a hybrid operating room equipped with a ceiling-mounted C-arm system with CBCT capabilities (Allura Xper FD20; Philips). At the time of the study, a formalized anesthesia protocol was not yet established and, therefore, anesthesia settings were variable per patient and were not recorded as part of this study. According to the study design, preprocedure CT images were imported into the LungVision software, where the physician identified the target lesion and selected the planned navigation pathway per manufacturer instructions. At the beginning of the procedure, a registration step was performed to correlate the preoperative CT scan with the patient's positioning during the procedure. The target lesion and pathway were displayed as an overlay on live fluoroscopy views throughout the procedure. A flexible bronchoscope (BF-1T180; Olympus) was

navigated to the target lobe and a fluoroscopically visible, steerable catheter (Edge Firm Tip; Medtronic) was introduced through the bronchoscope working channel. The catheter, without any electromagnetic components, was guided to the electronically highlighted target by following the pathway overlaid on the fluoroscopic image. When the display showed the catheter tip positioned at the lesion, a CBCT scan was acquired to verify catheter tip localization (it was not used to aid in obtaining a diagnosis). Once verified, multiple biopsy tools, including a needle, standard cytology brush, biopsy forceps, needle cytology brush, and bronchoalveolar lavage, were used according to physician preference. Rapid on-site cytopathologic examination was performed by a cytotechnologist and cytopathologist present in the operating room. One-year follow-up data was collected to confirm final diagnosis in those who had a nondiagnostic index procedure.

The primary outcome was lesion localization success, defined as the tip of the catheter visualized within the confines of the lesion as displayed on augmented fluoroscopic view and confirmed by CBCT at the end of navigation. When the lesion was reached, the catheter was confirmed in multiple

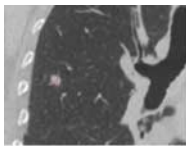
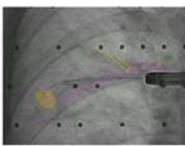
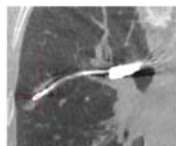
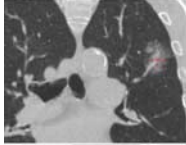
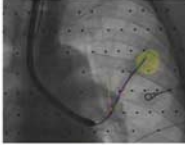
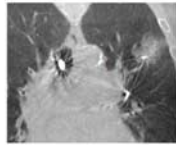
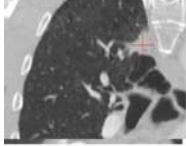
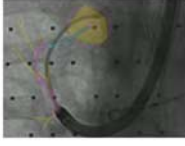
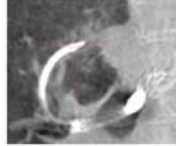
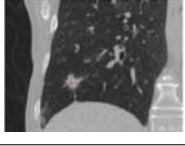
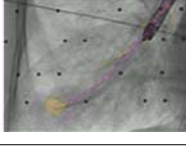
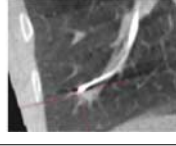
Lesion Location	Lesion Size (mm)	CT Image	Navigation Pathway	CBCT Confirmation	Accuracy (mm)
RUL	8.0				2.1
LUL	18.0				3.1
RUL	18.0				5.2
RLL	11.0				11.4

FIGURE 2. Real-time target verification by cone-beam computed tomography (CBCT) and accuracy measurements. From left to right columns: peripheral pulmonary lesions (PPLs) marked on a computed tomography (CT) image. A proposed pathway was presented by the system, and the physician navigated with a steerable catheter through the working channel of the bronchoscope to the lesion according to the highlighted pathway. Once the catheter reached the proposed PPL location, localization to the marked lesion (highlighted in yellow) was confirmed by a CBCT scan. Accuracy measurements of the distance between the center of the PPL provided by the augmented system display to the PPL center as shown by CBCT scan were calculated. LUL indicates left upper lobe; RLL, right lower lobe; RUL, right upper lobe.

orthogonal fluoroscopic views to be present within the lesion (Fig. 2, CBCT confirmation column, first row) or at the edge of the lesion in a location that would allow biopsy without further maneuvers (Fig. 2, CBCT confirmation column, third image from the top). Lesion localization accuracy was measured as the distance between the center of the lesion as shown on augmented fluoroscopic view and the center of the lesion as shown on CBCT. CBCT was only used for accuracy measurements and determination of localization success; it was not used to aid in obtaining a diagnosis. R-EBUS was not used in this study.

Consistent with the AQuIRE registry definition,⁸ a bronchoscopy procedure in our study was only considered diagnostic if the lesion was either malignant or specifically benign, based on the index procedure. If findings were nonspecific (ie, inflammatory changes), the procedure was considered nondiagnostic. Such lesions were then characterized as indeterminate and followed with serial CT scans if the patient was not suitable for a more invasive diagnostic procedure. A bronchoscopy result that showed malignancy was considered a true positive (TP). A definitive nonmalignant diagnosis obtained from the bronchoscopy and correlated with clinical findings was considered a true negative (TN). Diagnostic yield was calculated both per patient and per lesion as the number of lesions with a definitive histologic diagnosis (malignant or benign) obtained during the index procedure, divided by the number of lesions biopsied (TP+TN/total of lesions biopsied). Diagnostic yield was assessed for all lesions and separately for lesions ≤ 20 and > 20 mm in diameter.

Patients with indeterminate lesions after the initial bronchoscopy were followed and managed according to the physician's judgment to determine a definitive diagnosis. Follow-up data were collected up to 12 months postprocedure and used to measure diagnostic accuracy (defined as 12-month diagnostic yield in the NAVIGATE study⁹). Patients with subsequent diagnostic tests confirming a nonmalignant diagnosis or without lesion progression on radiographic follow-up as of 12 months were considered TN. If the initial bronchoscopy was indeterminate and malignancy was eventually diagnosed during follow-up, or if the lesion increased in size on follow-up CT scans and the patient underwent definitive treatment for malignancy, the original finding was considered a false negative (FN). Diagnostic accuracy was calculated as the sum of malignant lesions, benign lesions, and indeterminate lesions confirmed as benign after follow-up, divided by the total number of lesions biopsied.

Prevalence of malignancy was calculated as the number of malignant results obtained on the day of the procedure, or at follow-up, divided by the total number of procedures performed. Sensitivity for malignancy [TP/(TP+FN)] and specificity of LungVision augmented fluoroscopy [TN/(TN+FP)] were also calculated. Two subjects did not have complete follow-up; therefore, a sensitivity analysis was conducted to determine the minimum sensitivity for malignancy (where subjects with incomplete follow-up were considered FN) and maximum sensitivity for malignancy (where subjects with incomplete follow-up were considered TN).¹²

CT-to-body divergence was measured using pre-procedural CT images and intraprocedural CBCT images taken immediately after intubation, aligned on the basis of the central airways. The distance between lesion centers in the *X*, *Y*, and *Z* directions was measured as a vector and actual CT-to-body divergence was calculated as $d = \sqrt{(x^2 + y^2 + z^2)}$.

Intraprocedural CBCT scans were evaluated for the presence of atelectasis and compared with preprocedural CT scans, which served as a baseline.

Complications were defined as bleeding requiring intervention (beyond standard suctioning), pneumothorax, respiratory failure postprocedure, and postprocedure hospitalization.

RESULTS

Augmented fluoroscopic guidance that provides visualization of both lesion and pathway was used to navigate to and biopsy PPLs in 53 patients. Seven patients had a second lesion evaluated on the same day, for a total of 60 target lesions. Three lesions in 2 patients who were lost to follow-up were excluded from the analysis (Fig. 3).

Fifty-seven percent of patients were men, the median age was 72 years (range: 46 to 85 years), and 84.3% of patients were current or former smokers. Most lesions (73.7%) were located in the upper lobes and 50% of lesions had a bronchus sign. The median lesion diameter was 18 mm (range: 7.0 to 48.0 mm), and 34 navigations (60.0%) were to lesions ≤ 20 mm in diameter. The average procedure time (scope in to scope out, not including staging endobronchial ultrasound) was 47 minutes. Pneumothorax, respiratory failure or bleeding events did not occur in any patients.

Successful navigation with LungVision was performed in 49 of the 51 patients for a total of 54 lesions, resulting in a lesion localization success rate

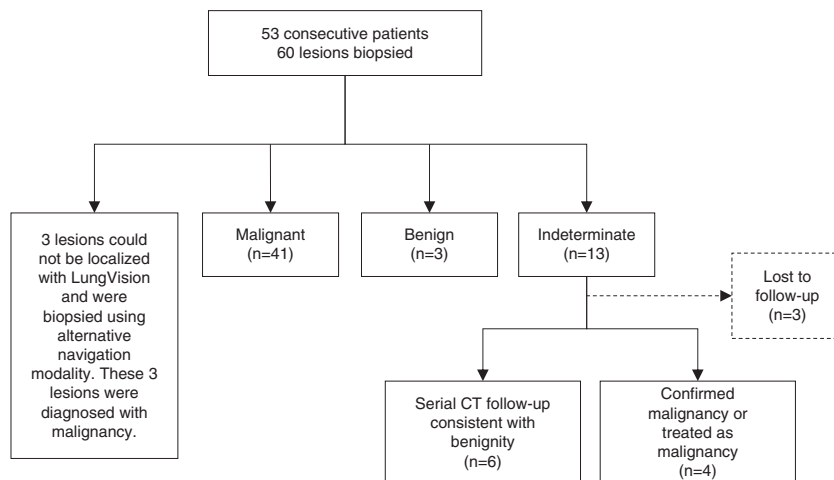


FIGURE 3. Flowchart of the study. Diagnostic yield per lesion was calculated by dividing the malignant lesions (n = 41) and the benign lesions (n = 3) by the total number of lesions (n = 57), resulting in a diagnostic yield per lesion of 77.2%. CT indicates computed tomography.

of 96.1% per patient and 94.7% per lesion (Table 1). Three navigations were unsuccessful due to system failure that could not calculate lesion location and provide a pathway to the lesion. In these cases, the physician reached the lesions with an alternate

standard-of-care navigation modality, and the malignant diagnoses obtained in these procedures were not counted toward the diagnostic yield of the system. Tissue biopsies were collected, and rapid on-site cytopathologic examination was performed

TABLE 1. Target Location Accuracy, Diagnostic Yield* and Diagnostic Accuracy†

Parameters	Results Per Patient (N = 51) [n (%)]	Results Per Lesion (N = 57) [n (%)]
Localizations confirmed by cone-beam CT	49 (96.1)	54 (94.7)
Diagnostic yield (at the day of procedure)	40 (78.4)	44 (77.2)
Lesions ≤ 20 mm	21 (70.0)	24 (70.6)
Lesions > 20 mm	19 (90.5)	20 (87.0)
Diagnostic accuracy (after follow-up)	45 (88.2)	50 (87.7)
Minimum sensitivity for malignancy‡	86.7%	86.3%
Maximum sensitivity for malignancy§	95.2%	91.7%
Specificity	100.0%	100.0%
Prevalence of malignancy on the day of procedure	37 (75.5)	41 (75.9)
Prevalence of malignancy after follow-up	41 (83.7)	45 (83.3)
Diagnosis	Lesions ≤ 20 mm (N = 34) [n (%)]	Lesions > 20 mm (N = 23) [n (%)]
Adenocarcinoma	16 (47)	8 (35)
Squamous cell carcinoma	5 (15)	7 (31)
Non-small cell carcinoma	1 (3)	3 (13)
Sarcomatoid carcinoma	0	1 (4)
Neuroendocrine tumor	1 (3)	0
Metastatic melanoma	1 (3)	1 (4)
Infection	2 (6)	0
Granulomatous inflammation	1 (3)	0
Reactive radiation effect	1 (3)	0
Nondiagnostic	6 (17)	3 (13)

Lesion localization was confirmed by cone-beam computed tomography scans when the guided catheter was located within or at the edge of the lesion at the end of navigation.

*Diagnostic yield of procedures localized with LungVision was calculated as definitive histologic diagnosis (malignant and benign) at the day of the procedure.

†Diagnostic accuracy of procedures localized with LungVision was calculated as malignant and benign lesions and indeterminate lesions confirmed as benign after 12 months follow-up divided by the total number of lesions biopsied.

‡Minimum sensitivity was based on the assumption that patients with uncompleted follow-up (n = 3) had lung cancer (ie, false negative).

§Maximum sensitivity was based on the assumption that patients with uncompleted follow-up (n = 3) did not have lung cancer (ie, true negative).

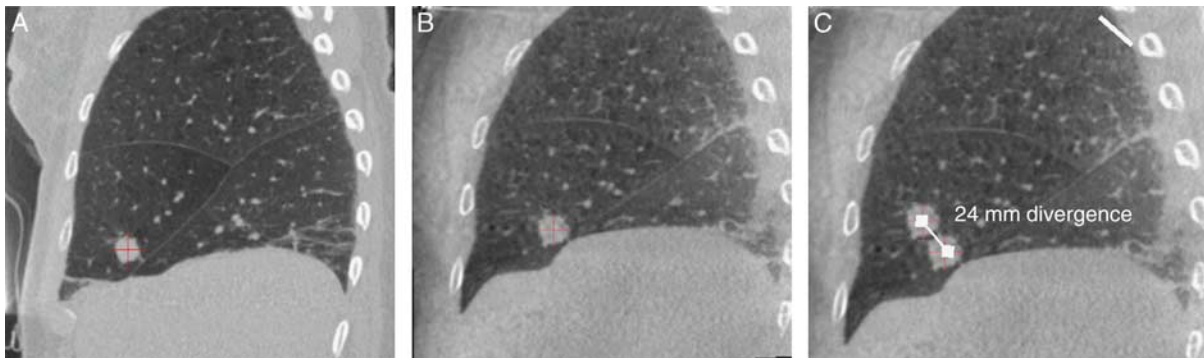


FIGURE 4. Computed tomography (CT)-to-patient divergence measurements. Sagittal view of a suspicious lesion on a preprocedural CT image (A), an interprocedural cone-beam CT scan (B), and an illustration of the distance, measured in 3-dimensions (C), between lesion centers on the preprocedure CT image compared with intraprocedure cone-beam CT image. In this procedure the CT-to-body divergence measured was 24 mm. **u+**

for all 51 patients (54 lesions). The diagnostic yield was 78.4% per patient and 77.2% per lesion (Table 1). Diagnostic yield was 70.6% for lesions ≤ 20 mm in diameter and 87.0% for lesions > 20 mm in diameter.

During the index procedure, malignancy was diagnosed in 41 lesions, based on final pathology results. The prevalence of malignancy was 75.9%. At 12-month follow-up, malignancies were confirmed in 45 lesions resulting in prevalence of malignancy of 83.3% at follow-up. Four indeterminate results at the index procedure were subsequently diagnosed as malignant in follow-up procedures and were counted as FN (Fig. 2). Per lesion, the maximum sensitivity for malignancy was 91.7%. Specificity was 100%, and diagnostic accuracy for all lesion types (malignant, benign, or indeterminate) was 87.7%.

The distance between lesion location shown on the LungVision system at the end of navigation compared with lesion location shown on CBCT (average localization accuracy) was 5.9 mm (range: 2.1 to 10.0 mm). Average localization accuracy by lesion location is shown in Figure 2. The average CT-to-body divergence was 14.5 mm (range: 2.6 to 33.0 mm) overall, 13.0 mm (range: 2.6 to 33.0 mm) in the upper lobes and 21.9 mm (range: 10.0 to 29.0 mm) in the nonupper lobes (Fig. 4).

Atelectasis was identified to varying degrees in approximately half of the procedures. Corresponding images of preoperative CT, CBCT prenavigation and CBCT postnavigation depicting atelectasis during bronchoscopy are shown in Figure 5.

DISCUSSION

Use of this novel endobronchial augmented fluoroscopic navigation system with real-time

visualization of PPLs during biopsy resulted in a high lesion localization success rate (96.1%) and high localization accuracy (mean 5.9 mm) as verified by CBCT at the end of navigation in all patients. Sensitivity for malignancy was high, with biopsies obtained from the system correctly identifying malignancy during the procedure in 91.7% of lesions later determined to be malignant at follow-up procedures. Overall, diagnostic accuracy was also high (87.7%).

Accurate localization of PPLs is important for acquiring informative biopsy samples during bronchoscopy. Navigation modalities, such as ENB, virtual bronchoscopy and robotic bronchoscopy with either ENB or shape-sensing guidance, have shown high localization success, but diagnostic yield has not risen in parallel. Diagnostic yield was 38.5% with ENB alone in the AQUIRE registry⁸ and 69.1% in a recent retrospective multicenter report of ENB-guided robotic bronchoscopy.¹³ These modalities all use a virtual pathway and target calculated based on preoperative CT images during navigation to guide the physician to the lesion, and in many procedures, this approach does not reflect the actual lesion location. Newer technologies have aimed to correct for CT-to-body divergence using real-time imaging. A single-center, retrospective study of the first experience with fluoroscopic ENB consisting of digital tomosynthesis with a conventional C-arm that allows local re-registration of the lesion at the end of navigation showed an improved diagnostic yield of 79% compared with standard ENB (59%).¹⁴

Real-time visualization of the target lesion during bronchoscopy is helpful for procedural success, as it allows the physician to track lung motion


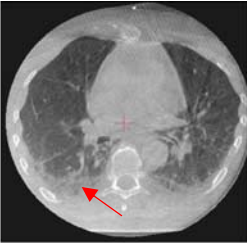
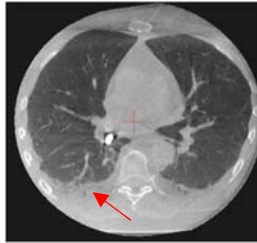
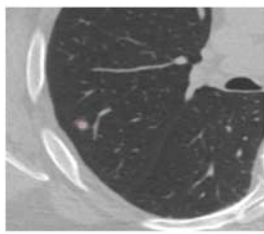


Lesion Location	Lesion Size	Divergence Measured	CT	CBCT Pre	CBCT Post
RLL	15 mm	25.8 mm			
RUL	9 mm	24.0 mm			

FIGURE 5. Atelectasis identified during bronchoscopy. Corresponding images of computed tomography (CT), cone-beam computed tomography (CBCT) preprocedure, and CBCT postprocedure show atelectasis (denoted by red arrows) during bronchoscopy. Atelectasis was identified in half of the procedures. RLL indicates right lower lobe; RUL, right upper lobe. **u+**

and thus “lesion motion” while navigating within the bronchial tree to a peripheral lesion. Lung volumes, airway orientation and catheter location within the lungs change constantly as a result of breathing motion. Movement of pulmonary lesions at full inspiration on planning chest CT scan relative to end exhalation during tidal volume breathing may significantly affect the diagnostic yield of ENB.¹⁵ Chen et al¹⁵ reported average pulmonary lesion movement resulting from respiratory motion of 17.6 mm.

R-EBUS can provide real-time confirmation of lesion location but does not provide guidance for navigation to the lesion or guidance on accessing the lesion. R-EBUS has demonstrated high lesion localization rates during bronchoscopy, but without corresponding high diagnostic yield.^{8,16–18} Chen et al¹⁹ reported a high localization rate (97%) but low diagnostic yield (58.9%) in their single-center study using a CT-anatomic correlation with multiplanar CT scan reconstruction and R-EBUS verification to localize peripheral lesions. A number of factors can contribute to this mismatch, including limitations of biopsy tools; lesion size, location, and morphology; and lack of a bronchus sign.²⁰ Tanner and colleagues has also reported a low diagnostic yield of R-EBUS when combined with thin bronchoscope (49%) compared with diagnostic yield of

standard bronchoscopy (37%) in a multicenter, randomized study.⁵

CBCT is another modality that offers real-time visualization of the target lesion as well as proximity of catheter or biopsy tool. The information is provided in real-time during the procedure in the form of augmented fluoroscopy; however, the overlaid images on live fluoroscopy are static. Therefore, the true lesion location, as represented by the augmented fluoroscopic view, will be most accurate during a breath hold. In contrast, the LungVision system provides augmented fluoroscopy view of the actual lesion location in real-time during navigation and biopsy with continuous dynamic tracking of the pathway and target lesion.

Although the ability to localize the tip of the catheter within or at the edge of the virtual lesion is a critical step in successful biopsy of a PPL, if the technology is unable to compensate for CT-to-body divergence and breathing motion during the procedure, the biopsy tissue may be collected from a site that does not represent the true lesion location. As shown in our study, combined guidance of navigation and biopsy with real-time fluoroscopic visualization of the lesion and tools resulted in a higher diagnostic yield overall (78.4%) and for lesions ≤20 mm in diameter (71.0%), which accounted for 60% of the lesions biopsied.

As previously mentioned, CT-to-body divergence can result from differences between patient position during the preoperative CT scan and position during bronchoscopy, as well as from physiological variations occurring during the time between the 2 procedures. CT-to-body divergence has been shown to shift the expected location of PPLs during bronchoscopy from the location marked on the preoperative CT scan.²¹ Using CBCT, we measured average movement of 13 mm in the upper lobes and 22 mm in the nonupper lobes compared with the expected location on the preoperative CT images. This calculation was made before insertion of the bronchoscope or catheter. This issue is especially relevant when evaluating small lesions (≤ 20 mm) where the displacement distance can be larger than the diameter of the lesion itself, likely resulting in off-target biopsy attempts and lower diagnostic yield. Other physiological changes, such as atelectasis, also have an impact on visualizing the lesion. Casal et al²² described that in 20% of their reported cases, the target lesion was completely obscured due to atelectasis.

In this study, atelectasis was identified in approximately half of the procedures by comparing preoperative CT images with prenavigation and postnavigation CBCT images. A specific ventilation protocol was not used in this study. Atelectasis was identified to varying degrees in 1 or more lobes, usually in dependent portions of the lung bases and posteriorly, not necessarily in the vicinity of the lesion. Atelectasis, which can occur as a result of anesthesia, chest muscle weakness or paralysis, and hyperoxia,²³ was shown to contribute to significant changes in lesion position in many of the procedures (Fig. 5). Further studies are required to measure the impact of atelectasis on lesion location during bronchoscopy. We believe that the use of an “open lung” ventilation protocol to minimize atelectasis could increase diagnostic yield, as it reduces CT-to-body divergence.

In our study, diagnostic yield was shown to be dependent on lesion size, similar to a previous meta-analysis.¹⁶ The diagnostic yield was higher for lesions > 20 mm (87.0%) than for lesions ≤ 20 mm (71.0%). Diagnostic yield of 78.4% counted only cases with definitive malignant or benign diagnosis at the index procedure (consistent with the AQUIRE registry definition⁸) and diagnostic accuracy of 87.7% reflects diagnoses after 12 months follow-up including cases that were confirmed to be benign (consistent with the NAVIGATE study definition⁹). This compares

favorably with the AQUIRE diagnostic yields of 38.5% for ENB alone and 47.1% for ENB combined with R-EBUS,⁸ as well as the 73% diagnostic accuracy of ENB in NAVIGATE.⁹

This study has several limitations. All procedures and measurements were performed by a single physician at a single center, which limits the generalizability of the findings and introduces the possibility of selection bias. In addition, the LungVision system features were updated throughout the study as the algorithm was improved, such that not all procedures were performed using exactly the same software version. Patients were enrolled in the study without restrictions on lesion size, location, and stage of disease. Multicenter studies with multiple operators using the same software algorithm are needed to confirm these findings, as well as cost-effectiveness and efficiency studies.

CONCLUSIONS

With an excellent safety profile, high lesion localization rate, and improved diagnostic yield and sensitivity for malignancy, the LungVision augmented fluoroscopic navigation platform has the potential to enable safe, effective biopsies and accurate diagnosis of PPLs.

REFERENCES

1. Siegel RL, Miller KD, Jemal A. Cancer statistics, 2020. *CA Cancer J Clin.* 2020;70:7–30.
2. Blandin Knight S, Crosbie PA, Balata H, et al. Progress and prospects of early detection in lung cancer. *Open Biol.* 2017;7:170070.
3. Belanger AR, Akulian JA. An update on the role of advanced diagnostic bronchoscopy in the evaluation and staging of lung cancer. *Thorax.* 2017;72:211–221.
4. Schreiber G, McCrory DC. Performance characteristics of different modalities for diagnosis of suspected lung cancer: summary of published evidence. *Chest.* 2003;123(suppl):115S–128S.
5. Asano F, Eberhardt R, Herth FJ. Virtual bronchoscopic navigation for peripheral pulmonary lesions. *Respiration.* 2014;88:430–440.
6. Ozgul G, Cetinkaya E, Ozgul MA, et al. Efficacy and safety of electromagnetic navigation bronchoscopy with or without radial endobronchial ultrasound for peripheral lung lesions. *Endosc Ultrasound.* 2016;5:189–195.
7. Tanner NT, Yarmus L, Chen A, et al. Standard bronchoscopy with fluoroscopy vs thin bronchoscopy and radial endobronchial ultrasound for biopsy of pulmonary lesions: a multicenter, prospective, randomized trial. *Chest.* 2018;154:1035–1043.
8. Ost DE, Ernst A, Lei X, et al. Diagnostic yield and complications of bronchoscopy for peripheral lung lesions. Results of the AQUIRE Registry. *Am J Respir Crit Care Med.* 2016;193:68–77.
9. Folch EE, Pritchett MA, Nead MA, et al. Electromagnetic navigation bronchoscopy for peripheral

- pulmonary lesions: one-year results of the prospective, multicenter NAVIGATE study. *J Thorac Oncol*. 2019;14:445–458.
10. Hohenforst-Schmidt W, Zarogoulidis P, Vogl T, et al. Cone beam computer tomography (CBCT) in interventional chest medicine—high feasibility for endobronchial realtime navigation. *J Cancer*. 2014;5:231–241.
 11. Pritchett MA, Schampaert S, de Groot JAH, et al. Cone-beam CT with augmented fluoroscopy combined with electromagnetic navigation bronchoscopy for biopsy of pulmonary nodules. *J Bronchology Interv Pulmonol*. 2018;25:274–282.
 12. De Groot JA, Bossuyt PM, Reitsma JB, et al. Verification problems in diagnostic accuracy studies: consequences and solutions. *BMJ*. 2011;343:d4770.
 13. Chaddha U, Kovacs SP, Manley C, et al. Robot-assisted bronchoscopy for pulmonary lesion diagnosis: results from the initial multicenter experience. *BMC Pulm Med*. 2019;19:243.
 14. Aboudara M, Roller L, Rickman O, et al. Improved diagnostic yield for lung nodules with digital tomosynthesis-corrected navigational bronchoscopy: initial experience with a novel adjunct. *Respirology*. 2020;25:206–213.
 15. Chen A, Pastis N, Furukawa B, et al. The effect of respiratory motion on pulmonary nodule location during electromagnetic navigation bronchoscopy. *Chest*. 2015;147:1275–1281.
 16. Gex G, Pralong JA, Combescure C, et al. Diagnostic yield and safety of electromagnetic navigation bronchoscopy for lung nodules: a systematic review and meta-analysis. *Respiration*. 2014;87:165–176.
 17. Chen A, Chenna P, Loisel A, et al. Radial probe endobronchial ultrasound for peripheral pulmonary lesions. A 5-year institutional experience. *Ann Am Thorac Soc*. 2014;11:578–582.
 18. Gildea TR. Lung lesion localization and the diagnostic drop. *Ann Am Thorac Soc*. 2016;13:1450–1452.
 19. Chen AC, Loisel A, Zhou L, et al. Localization of peripheral pulmonary lesions using a method of computed tomography-anatomic correlation and radial probe endobronchial ultrasound confirmation. *Ann Am Thorac Soc*. 2016;13:1586–1592.
 20. Seijo LM, de Torres JP, Lozano MD, et al. Diagnostic yield of electromagnetic navigation bronchoscopy is highly dependent on the presence of a Bronchus sign on CT imaging: results from a prospective study. *Chest*. 2010;138:1316–1321.
 21. Pritchett MA. Augmented endobronchial fluoroscopic navigation and localization system: comparison with cone beam CT. A Poster Presentation. *Am J Respir Crit Care Med*. 2018;197:A6156.
 22. Casal RF, Sarkiss M, Jones AK, et al. Cone beam computed tomography-guided thin/ultrathin bronchoscopy for diagnosis of peripheral lung nodules: a prospective pilot study. *J Thorac Dis*. 2018;10:6950–6959.
 23. Rusca M, Proietti S, Schnyder P, et al. Prevention of atelectasis formation during induction of general anesthesia. *Anesth Analg*. 2003;97:1835–1839.